High-spin polaron in lightly doped CuO_2 planes

Bayo Lau, Mona Berciu, and George A. Sawatzky
Department of Physics and Astronomy, University of British Columbia, Vancouver, BC, V6T 1Z1
(Dated: January 17, 2011)

We derive and investigate numerically a minimal yet detailed spin polaron model that describes lightly doped CuO_2 layers. The low-energy physics of a hole is studied by total-spin-resolved exact diagonalization on clusters of up to 32 CuO_2 unit cells, revealing features missed by previous studies. In particular, spin-polaron states with total spin 3/2 are the lowest eigenstates in some regions of the Brillouin zone. In these regions, and also at other points, the quasiparticle weight is identically zero indicating orthogonal states to those represented in the one electron Green's function. This highlights the importance of the proper treatment of spin fluctuations in the many-body background.

PACS numbers: 71.10.Fd,75.10.Jm,71.38.-k,74.72.-h

Introduction: A full understanding of the physics of a CuO_2 layer doped with a few holes has still not been achieved, despite continuous effort [1, 2]. Recent high resolution angular resolved photoemission (ARPES) studies [3–5] on the insulating charge-transfer gap parent compounds [6] reveal major puzzles: do quasiparticles of one electron nature exist and if so what is their energy and momentum? Why are the first visible electron removal states so broad, of 300 meV at 300K and decreasing linearly with temperature T, and what causes the very apparent T-dependent change of line shapes? Is the momentum dependence of the lowest energy structure related to the pseudo-gap formation at higher hole concentrations? Recent neutron experiments performed in the pseudo-gap phase reported magnetic response throughout the Brillouin zone, not restricted to the region of the much discussed magnetic resonance [7]. These and other issues including the broken local 4-fold symmetry, which is taken for granted in single-band models, seen in scanning tunneling probe (STM)[8] and X-ray scattering [9] remain either open questions or are controversial.

It is widely believed that a complete description of a single hole in a spin-$\frac{1}{2}$ 2D antiferromagnet (AFM) with *full* quantum fluctuations could provide the answers to these questions, as well as clues for understanding the origin of the non-Fermi-liquid behavior and the superconducting ground-state in the higher hole density region. Of course, consideration of exotic many-body scenarios [10], or of coupling to lattice vibrations [11] are exciting developments; however, a detailed modeling of the hole+AFM is a crucial first step to understand the significance of such additions. This problem is very difficult because of the complicated nature of the 2D AFM background, whose quantum fluctuations in the presence of doped holes were never fully captured for a large CuO_2 lattice. Recent technical developments [12] allow us to present the first such results for samples with up to 32 Cu and 64 O, in this Letter. Our work also reveals important failings of the single-band models used extensively in the literature, and which we briefly review below [13].

Microscopic hole-AFM interactions have been studied in models with one [14–17], two [18–20], three [21], or more [22, 23] bands. While exact analytical solutions seem to be out of reach, numerical studies are always carried out with compromises such as the use of small clusters and variational approaches[24]. Given these difficulties and the drive to find the simplest model, the one-band models are unsurprisingly the most studied [14]. While certain higher-energy aspects observed by XAS, EELS and STM [2, 25] cannot be described using one band, the significance of omitting other bands in the low-energy scale cannot be quantified without a comparison to unbiased solutions of more detailed models.

Cuprates exhibit charge-transfer band-gap behavior with mobile holes located mainly on anion ligands and unpaired electrons on cation d-orbitals [6]. One-band models use superexchange [26] and Zhang-Rice singlets (ZRS) [15] to reduce the $(N-n)$-electron problem to one of n holes in an AFM background, often modeled as a Néel background with spin-waves. To reach agreement with experiments, such models must be tweaked at least by adding longer-range hopping [20, 27]. One trade-off for their elegance is the use of momentum-independent effective parameters, even though it is well known that the ZRS state has a strong $\mathbf{k}$-dependent renormalization [15]. The impact of such approximations must be verified for all $\mathbf{k}$ with models that distinguish anion and cation sites.

In this Letter we study a single hole in a model that includes the O $2p$ orbitals explicitly and *full quantum fluctuations* of the AFM background. This results in spin-polaron solutions absent from other models or approximations used to date. The energy dispersion of the lowest energy electron removal state is similar to that of the ZRS, which effectively locks the O hole in a singlet with *one of the two* adjacent copper sites. Without such restrictions, our resulting wavefunction features the hole forming a stable $S = \frac{1}{2}$ three-spin polaron (3SP) with its *two neighbour copper* sites. In some regions of the Brillouin zone, a $S = 1$ quantum fluctuation binds to the $S = \frac{1}{2}$ polaron yielding a low-energy $S = \frac{3}{2}$ state invisible at $T = 0$ to ARPES. For all momenta, the $S = \frac{3}{2}$ states are found to be within $\lesssim J/2$ of the $S = \frac{1}{2}$ band. These

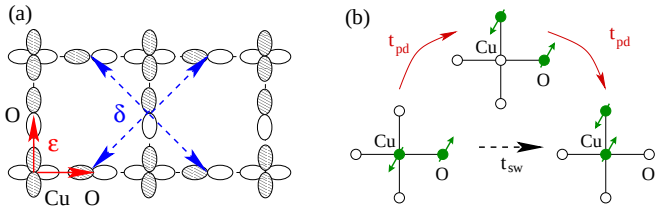

FIG. 1. (a) Two adjacent unit cells of the CuO_2 plane. The orbitals kept in the 3-band model of Eq. (1) are shown, with white/shaded for positive/negative signs. The two ϵ vectors (solid arrow) and the four δ vectors (dashed arrow) are also shown. (b) Sketch of a virtual process of $T_{\rm swap}$.

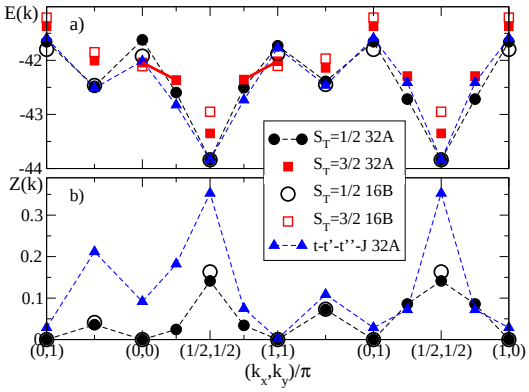

FIG. 2. a) Energy and b) quasiparticle weight (bottom) for the lowest eigenstates with $S_T = \frac{1}{2}$ and $\frac{3}{2}$ vs. momentum. Different sets are shifted so as to have the same GS energy.

and other results inconsistent with one-band models, and their experimental implications, are discussed below.

We start with the three-band $p-d$ model which exhibits the basic physics of a hole doped charge transfer gap and insulating spin 1/2 antiferromagnet [21]:

$$H_{3B} = T_{pd} + T_{pp} + \Delta_{pd}\sum n_{l+\epsilon,\sigma} + U_{pp}\sum n_{l+\epsilon,\uparrow}n_{l+\epsilon,\downarrow} + U_{dd}\sum n_{l,\uparrow}n_{l,\downarrow} \quad (1)$$

where $n_{l,\sigma} = d^\dagger_{l,\sigma}d_{l,\sigma}$, $n_{l+\epsilon,\sigma} = p^\dagger_{l+\epsilon,\sigma}p_{l+\epsilon,\sigma}$ count holes in Cu $3d_{x^2-y^2}$, respectively O $2p_{x/y}$ orbitals (see Fig. 1) and $U_{dd} > U_{pp} > \Delta_{pd}$ describe Hubbard and charge transfer interactions. Nearest neighbor (NN) Cu-O hopping $T_{pd} = t_{pd}\sum[(p^\dagger_{l+\epsilon,\sigma} - p^\dagger_{l-\epsilon,\sigma})d_{l,\sigma} + h.c.]$ is included, as is hopping $T_{pp} = t_{pp}\sum s_\delta p^\dagger_{l+\epsilon+\delta,\sigma}p_{l+\epsilon,\sigma} - t'_{pp}\sum(p^\dagger_{l-\epsilon,\sigma} + p^\dagger_{l+3\epsilon,\sigma})p_{l+\epsilon,\sigma}$ between NN and certain NNN O sites. For NN hopping by $\delta = (\delta_x, \delta_y)$, $s_\delta = \delta_x\delta_y/|\delta_x\delta_y|$.

In a half-filled, large-U system with *no hopping*, the ground-state (GS) has a hole at each Cu site: $\prod d^\dagger_{l,\sigma_l}|0\rangle = \prod|\sigma_l\rangle$, with the usual 2^N spin degeneracy. An electron removal adds a hole in an O orbital, so the doped GS is $p^\dagger_{l+\epsilon,\sigma}\prod|\sigma_l\rangle$, with $2N\times 2^{N+1}$ degeneracy. We study the behavior of such anion holes when the hopping is turned on, in the framework of superexchange. The idea is reminiscent of studies such as Refs. [18, 19, 22]; however, these also used further approximations. A detailed comparison of our Hamiltonian versus those used in these references is provided in the Supplementary Material [13].

Model: Noting that all T_{pd} processes increase energy by either U and/or Δ_{pd}, we derive the effective model for the states $p^\dagger_{l+\epsilon,\sigma}\prod|\sigma_l\rangle$ to be [13]:

$$H_{\rm eff} = T_{pp} + T_{\rm swap} + H_{J_{pd}} + H_{J_{dd}} \quad (2)$$

where the O-O hopping of the hole is supplemented by:

$$T_{swap} = -t_{sw}\sum s_\eta p^\dagger_{l+\epsilon+\eta,\sigma}p_{l+\epsilon,\sigma'}|\sigma'_{l_{\epsilon,\eta}}\rangle\langle\sigma_{l_{\epsilon,\eta}}| \quad (3)$$

$$H_{J_{pd}} = J_{pd}\sum \overline{S}_l\cdot\overline{S}_{l\pm\epsilon} \quad (4)$$

$$H_{J_{dd}} = J_{dd}\sum \overline{S}_{l\pm2\epsilon}\cdot\overline{S}_l\Pi_\sigma(1-n_{l\pm\epsilon,\sigma}) \quad (5)$$

Using $t_{pd} = 1.3eV$, $t_{pp} = 0.65eV$, $t'_{pp} = 0.58t_{pp}$, $\Delta_{pd} = 3.6eV$, and $U_{pp} = 4eV$ [14], we scale the parameters in units of J_{dd} to find their *dimensionless* values to be $t_{pp} = 4.13$, $t_{sw} = 2.98$, and $J_{pd} = 2.83$.

While we find that the 3-spin polaron (3SP) [19] plays an important role, our approach is different from previous work [18] by recognizing (i) T_{pp}'s role as a coherence facilitator rather than a mere correction; (ii) its complementing process T_{swap}, illustrated in Fig. 1(b), (iii) suppression of superexchange along the bond inhabited by the hole, see Eq. (5) [13], and iv) total-spin (S_T) eigenstates are studied explicitly. We push the computational limit to perform S_T-resolved exact diagonalization (ED) of a topologically superior [28] cluster of $N = 32$ CuO_2 unit cells, treating the AFM background exactly. ED provides the transparency, flexibility, and neutrality to support new results. The price for a systematic mapping of the excited states is the limited $\mathbf{k}$ resolution. $N = 16$ results are provided to check for size dependence.

We find that all low-energy eigenstates have a total spin of either $S_T = \frac{1}{2}$ or $\frac{3}{2}$. The z-projections for each S_T are degenerate. The $S_T = \frac{1}{2}$ subspace is due to the $s = \frac{1}{2}$ hole mixing with various $S = 0$ background states, including the AFM GS, or mixing with the $S = 1$ background states, including the "single-magnon" states. The $s = \frac{1}{2}$ carrier can also mix with $S = 1$ or 2 background states to yield the $S_T = \frac{3}{2}$ subspace; we explicitly consider such states here for the first time. The partition of the S^z_T subspace into separate S_T sectors was managed by the optimizations of Ref. [12]. Unlike there, *no basis truncation* was employed here for rigorous results. The $(\mathbf{k}, S_T = \frac{3}{2}, S^z_T = \frac{1}{2})$ sector contains $\sim 0.44\times10^9$ states.

Results: Fig. 2(a) shows the lowest eigenenergies. The GS has $\mathbf{k} = (\frac{\pi}{2}, \frac{\pi}{2})$ and $S_T = \frac{1}{2}$, is consistent with the 3SP but can also be thought of in terms of ZRS [13]. Remarkably, we find similar dispersion along (0,0)→(π,π) and (0,π)→(π,0) without having to add longer range hopping or fine-tune parameters as is needed in one band models. The biggest surprise, though, are the low-lying $S_T = \frac{3}{2}$ states which go below the $\frac{1}{2}$ states near (0,0)

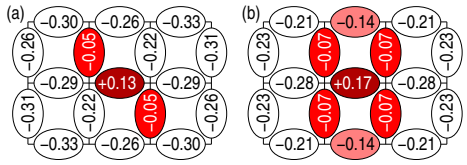

FIG. 3. $\langle C_x(\delta,a)\rangle$ for the lowest energy state at (a) $(\frac{\pi}{2},\frac{\pi}{2})$ with $S_T=\frac{1}{2}$, and (b) at (π,π) with $S_T=\frac{3}{2}$. The darkly-shaded bullet denotes the oxygen position at $l+e_x$. Each bullet shows the correlation value between the two sandwiching Cu sites. The central 12 Cu sites are shown; the correlations between the other 20 Cu spins converge fast towards the AFM value of ∼-0.33. $\langle C_y(\delta,a)\rangle$ is the $\hat{P}_{x\leftrightarrow y}$ reflection.

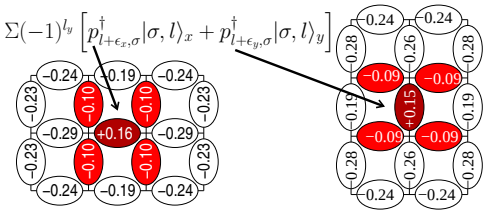

FIG. 4. $\langle C_{x/y}(\delta,a)\rangle$ for lowest state at k=$(0,\pi)$ with S_T=1/2.

and (π,π). Finite-size analysis, discussed in the Supplementary Material, reveals that the $S_T=\frac{3}{2}$ states are stable polarons at least in the regions marked by thick solid lines in Fig. 2(a). Thus, *a $S_T=\frac{1}{2}$ quasiparticle cannot describe the low-energy states throughout the BZ.* To compare the lowest energy states on both sides of the crossing, we note that the lowest $k_x=k_y$ eigenstates have odd parity upon a $\hat{P}_{x\leftrightarrow y}$ reflection (Fig.1a) so they can be expressed as $2^{-1/2}(1+\hat{P}_{x\leftrightarrow y})\sum e^{ikl}p^\dagger_{l+e_x,\sigma}|\sigma,l\rangle_x$. The band-crossing results in noticeable change in the expectation values of the correlation function:

$$\hat{C}_x(\delta,a)=2\sum_{l,\sigma}\overline{S}_{l+\delta}\cdot\overline{S}_{l+\delta+a}n_{l+e_x,\sigma} \qquad (6)$$

which measures the correlation between two neighboring Cu spins at a distance δ from the hole. $\langle C\rangle$ ranges from -3/4 for singlet, to ∼-0.33 for 2D AFM, to 1/4 for triplet.

Fig. 3a shows $\langle\hat{C}_x\rangle$ when the hole is located at the darkly shaded bullet, in the GS: $\mathbf{k}=(\frac{\pi}{2},\frac{\pi}{2})$, $S_T=\frac{1}{2}$ ($\langle\hat{C}_y\rangle$ is a reflection with $\hat{P}_{x\leftrightarrow y}$ for $k_x=k_y$). The hole affects the AFM order in its vicinity. Because of the hole-spin exchange $H_{J_{pd}}$ and the blocked superexchange between the two Cu spins neighboring the hole, these "central" spins have triplet correlations, of ∼0.13. Also, $\langle H_{J_{pd}}\rangle$ ∼ -0.9J_{pd}, showing that locally this is consistent with the 3SP solution [13]. More interesting are the correlations with the other 3 neighbors of each of these central Cu spins: with two of them, there are robust AFM correlations of ∼ −0.22, while with the third the correlation nearly vanishes (lightly shaded bullet). This is counterintuitive if one views the system as a fluctuating Neél background, where a spin-flip would change the spin-spin correlation to all four neighbors. Although the two central Cu spins have $\frac{2}{3}$ weight in triplet configuration which is hardly bi-partite, long-range AFM order cannot be automatically discounted [29]. Indeed, the correlations we find are consistent with such order, except for the zigzag of 3 bonds shown by shaded bullets. This strange shape is dictated by the hopping mechanism. For a Bloch wave, O-O hole hopping in the upper-left/lower-right direction yields a phase shift of $e^{i0}/e^{i(k_x-k_y)}$ and hence constructive interference if $k_x=k_y$. In contrast, hopping in the upper-right/lower-left direction yields a phase shift of e^{ik_x}/e^{-ik_y}, and the interference is scaled down by $\cos(k_{x/y})$. In the GS, having a mixture of singlets and triplets upper-left/lower-right to the O hole lowers energy with the least disturbance to AFM order. Thus, the two outside zigzag bonds are triplet "disturbance tails" pointing orthogonal to the momentum direction. This is very different from the ZRS, which freezes a Cu spin by intraplaquette coherence with its four O sites.

Fig. 3b shows the correlation values when the $S_T=\frac{3}{2}$ polaron becomes the lowest energy state at (π,π). The results look similar at (0,0). $\langle H_{J_{pd}}\rangle$ remains ∼ $-0.9J_{pd}$, but there are now four more heavily disturbed bonds. This further supports this being a stable polaron with an extra magnon bound locally close to the O hole. We stress here that this $\frac{3}{2}$ polaron is formed by a spin disturbance *around* the 3SP. This is very different from the $S=\frac{3}{2}$ excitation local to $H_{J_{pd}}$ with energy $+\frac{J_{pd}}{2}$ [22].

Fig. 2b shows the quasiparticle weight $Z(\mathbf{k})$ for the first electron removal state. The major difference from other models is that $Z(\mathbf{k})=0$ in three regions: a) $Z(0,0)=Z(\pi,\pi)$=0 because here the lowest eigenstate has $S_T=\frac{3}{2}$ which due to spin-conservation is not in the Krylov space of any $S_T=\frac{1}{2}$ state [13], and b) $Z(0,\pi)$=0 even though this is a $S_T=\frac{1}{2}$ state (see below). The t-t'-t"-J model treatment does not conserve S_T, resulting in $Z(0,0)\sim 0.1$ and a finite $Z(\pi,\pi)$ [16]. Our $Z(k)$ is smaller everywhere than that of the t-t'-t"-J model, suggesting less "free particle" nature of the polaron.

The lowest energy state at $\mathbf{k}=(0,\pi)$ has $S_T=\frac{1}{2}$, but its $Z=0$ because the state is not in the Krylov space of an electron removal [13]. This seems to be due to symmetry, although we do not yet fully understand this. States with finite but small Z are at least 0.006J higher in energy. Their close existence above the $Z=0$ lowest state may be related to pseudogap phenomena in this region; however, this needs to be investigated in more detail. Fig. 4 shows the correlation for this $Z=0$ lowest state. Compared to the GS (see Fig. 3a), there are 2 more disturbed bonds as required by the reflection parity about k. This larger disturbance range is accompanied by more negative (AFM) correlation values.

Although we are restricted to rather low momentum resolution, more can be said about the $E_{\frac{3}{2}}-E_{\frac{1}{2}}=0$ band crossings in the nodal direction by looking at the

k points between which the difference switch signs. The observation in Fig. 2a is that, going away from the $(\frac{\pi}{2},\frac{\pi}{2})$ GS, $E_{\frac{3}{2}}-E_{\frac{1}{2}}$ is larger towards $(0,0)$ than towards (π,π). The $\frac{1}{2}\rightarrow\frac{3}{2}$ band crossing would induce an *abrupt change in Z(k) from non-zero to exactly zero, irrespective of the $Z(k)$ value on the finite side.* The larger $E_{\frac{3}{2}}-E_{\frac{1}{2}}$ towards $k=(0,0)$ suggests that the non-zero region extends more towards $k=(0,0)$ than towards $k=(\pi,\pi)$. Fig. 2a also shows that the $\frac{3}{2}$ states get pushed further down as $N\rightarrow\infty$ so *the crossing is expected to be closer to the $(\frac{\pi}{2},\frac{\pi}{2})$ GS.* This is consistent with ARPES which indeed observed an abrupt peak suppression in the nodal direction as well as the peaks surviving longer towards $k=(0,0)$ [5].

Even when the $S_T=\frac{3}{2}$ states are not lowest in energy, they hug the $S_T=\frac{1}{2}$ band. This provides a $\lesssim J_{dd}/2$ energy scale for spin excitations. At finite T, as magnons become thermally activated, these $\frac{3}{2}$ states become "visible" to ARPES. This suggests a T-dependent broadening mechanism of $\lesssim J_{dd}/2$ scale, which, coincidentally, is the same energy scale recently linked to phonons, as another possible source for this broadening [4, 11].

Recent neutron experiments on samples at higher doping reveal $\sim 50meV$ magnetic response centered at q=0, away the AFM resonance momentum [7]. The bottom of the single-particle band structure in Fig 2a) indeed has a q=0 1/2-to-3/2 excitation of this energy scale. Our results so far are restricted to a single hole; nevertheless, it has been pointed out that the q=0 magnetic excitation can be explained by involving spins on oxygen sites [30], which certainly are present in our results.

In addition to the low-energy 3/2 polaron band, there are internal energy scales of the local 3SP since $H_{J_{PD}}$ also has a $S=\frac{1}{2}$ doublet and a $S=\frac{3}{2}$ quartet separated in energy by J_{pd} and $3J_{pd}/2$ from the lowest energy state. Magnetic excitations of these energy scales have been observed via inelastic resonant X ray scattering even for doped samples without long-range AFM order [31].

Summary: We solved a detailed model which includes the O sites and takes full account of the AFM quantum fluctuations, for large $N=32$ clusters. The phases of the p and d orbitals lead to phase coherence via $T_{pp}+T_{swap}$ [13]. This is re-enforced by $H_{J_{pd}}$ and the blocking of the AFM superexchange, making corrections such as T_{Kondo} negligible. While the dispersion is similar to that measured by ARPES without any fine-tuning, the lifting of Cu-O singlet restriction present in ZRS-based models leads to wavefunctions of different nature, i.e. the 3SP where the O hole correlates with both its neighbour Cu sites. This model also provides low-energy channels for $S=1$ excitations. $Z(k)$ was found to be identically zero in certain regions of the BZ for two reasons: 1) the spin-$\frac{3}{2}$ of the lowest energy state close to $(0,0)$ and (π,π); and 2) around the antinodal region because of the lowest energy state there being exactly orthogonal to the single electron removal state. The detailed nature of the state in the anti-nodal region is still being investigated.

Acknowledgement: We thank G. Khaliullin for discussions, B. Keimer for providing x-ray data, I. Elfimov and Westgrid for tech support, and CFI, CIfAR, CRC, NSERC and Sloan Foundation for funding.

[1] D. Bonn, Nature Physics **2**, 159 (2006;) S. Hufner *et al.*, Rep. Prog. Phys. **71**, 062501 (2008); D. M. Newns and D. Tsui, Nature Physics **3**, 184 (2007); G. Sangiovanni *et al.*, Phys. Rev. Lett. **97**, 046404 (2006); C. Webber *et al.*, Phys. Rev. Lett. **102**, 017005 (2009).
[2] M. Vojta, Advances in Physics **58**, 699 (2009).
[3] A. Damascelli *et al.*, Rev. Mod. Phys **75**, 473 (2003).
[4] K. M. Shen *et al.*, Phys. Rev. Lett. **93**, 267002 (2004); K. M. Shen *et al.*, Phys Rev B **75**, 075115 (2007).
[5] F. Ronning *et al.*, Phys. Rev. B **67**, 035113 (2003); F. Ronning *et al.*, Phys. Rev. B **71**, 094518 (2005).
[6] J. Zaanen, et al,Phys. Rev. Lett. **55**, 418 (1985).
[7] G. Yu *et al.*, Phys. Rev. B **81**, 064518 (2010). Y. Li *et al.* Nature 468 283 (2010)
[8] M. J. Lawler, et. al. Nature 466 347 (2010)
[9] P. Abbamonte, et. al. Nature Phys. 1 155 (2005)
[10] C. Varma, Nature 468 184 (2010).
[11] V. Cataudella *et al.*, Phys. Rev. Lett **99**, 226402 (2007).
[12] B. Lau *et al.*, Phys Rev B **81**, 172401 (2010).
[13] See Supplementary Material for more details.
[14] M. Ogata and H. Fukuyama, Rep. Prog. Phys. **71**, 036501 (2008); P. A. Lee, Rep. Prog. Phys. **71**, 012501 (2008).
[15] F.C. Zhang et al, Phys. Rev. B **37**, 3759 (1988).
[16] P. W. Leung *et al.*, Phys. Rev. B **56**, 6320 (1997).
[17] A. F. Barabanov *et al.*, JETP Letters **75**(2), 107 (2002).
[18] J. Zaanen and A. M. Oles, Phys. Rev. B **37**, 9423 (1988); D. M. Frenkel *et al.*, ibid **41**, 350 (1990); J.L. Shen et al, ibid **41**, 1969 (1990); H. Q. Ding *et al.*, ibid **46,** 14317 (1992); Y. Petrov and T. Egami, ibid **58**, 9485 (1998).
[19] V. J. Emery and G. Reiter, Phys. Rev. B **38**, 4547 (1988).
[20] A. Macridin *et al.*, Phys. Rev. B **71**, 134527 (2005); J.F. Annett and R. M. Martin Phys. Rev. B **42**, 3929 (1990); R. Eder and K. W. Becker, Z. Phys. B. **79**, 333 (1990);
[21] V. J. Emery, Phys. Rev. Lett. **58**, 2794 (1987); H. Eskes and G. A. Sawatzky, Phys. Rev. Lett. **61**, 1415 (1988).
[22] L. Klein and A. Aharony Phys. Rev. B **45**, 9915 (1992).
[23] D. F. Digor *et al.*, Theor. and Math. Phys. **149**, 1382 (2006). L. Hozoi *et al.*, Phys. Rev. B **75**, 024517 (2007); C. H. Patterson, Phys. Rev. B **77**, 094523 (2008); L. Hozoi *et al.*, Phys. Rev. B **78**, 165107 (2008).
[24] T. Yanagisawa *et al.*, Phys. Rev. B **64** 184509 (2001); J. Bonca *et al.*, Phys. Rev. B **76**, 035121 (2007); F. Tan and Q. H. Wang, Phys. Rev. Lett. **100**, 117004 (2008).
[25] M. Merz, Phys. Rev. Lett. **80** 5192 (1998); R. Schuster, Phys. Rev. B **79**, 214517 (2009).
[26] P. W. Anderson, Phys. Rev. **115**, 2 (1959).
[27] J.H. Jefferson *et al.*, Phys. Rev. B. **45**, 7959 (1992); O. P. Sushkov *et al.*, Phys. Rev. B. **56**, 11769 (1997).
[28] D.D. Betts *et al.*, Can. J. Phys. **77**, 353 (1999).
[29] S. Liang *et al.*, Phys. Rev. Lett. **61**, 365 (1988); R. Eder, Phys. Rev. B. **59**, 13810 (1999).
[30] B. Fauque, et al, Phys. Rev. Lett. 96 197001 (2006)
[31] B. Keimer, unpublished.